American Mineralogist, Volume 90, pages 679–686, 2005

The order-disorder character of $FeOHSO_4$ obtained from the thermal decomposition of metahohmannite, $Fe_2^{3+}(H_2O)_4[O(SO_4)_2]$

GENNARO VENTRUTI,[1] FERNANDO SCORDARI,[1] EMANUELA SCHINGARO,[1] ALESSANDRO F. GUALTIERI,[2] AND CARLO MENEGHINI[3]

[1]Dipartimento Geomineralogico, Università di Bari, I-70125 Bari, Italy
[2]Dipartimento di Scienze della Terra, Università di Modena e Reggio Emilia, I-41100 Modena, Italy
[3]Dipartimento di Fisica "E.Amaldi", Università di RomaTre, I-00146 Roma, Italy

ABSTRACT

The iron sulfate $FeOHSO_4$ studied was obtained as a dehydration product of metahohmannite $Fe_2(H_2O)_4[O(SO_4)_2]$ during a synchrotron real-time powder diffraction experiment. As quoted in the literature, $FeOHSO_4$ has iron atoms octahedrally coordinated with two hydroxyl groups and four sulfate O atoms, while each hydroxyl group is bonded to two iron atoms. This compound is commonly described in the orthorhombic system with space group *Pnma*, lattice parameters $a_J = 7.33$, $b_J = 6.42$, and $c_J = 7.14$ Å (a_J, b_J, and c_J are the Johansson lattice parameters), and $Z = 4$. However a preliminary Rietveld refinement of the pattern at about 220 °C using the structural model from the literature yielded a poor fit of the observed data and a final R_p value of about 23%. A careful analysis of the calculated powder diffraction pattern showed unexpected peaks, not observed in the experimental trace, for $h = 2n + 1$, while sharp reflections for $h = 2n$ seemed to point to different lattice constants and space group. The recognition of the order-disorder character of the $FeOHSO_4$ compound was the key to successfully interpreting the unexpected features of the experimental powder pattern and the misfit with respect to the calculated pattern. In fact, $FeOHSO_4$ belongs to a family of OD structures formed by equivalent layers of symmetry *Pbmm*. Only two MDO (Maximum Degree of Order) polytypes are possible. MDO1 results from a regular alternation of stacking operators $2_{1/2}$ and $2_{-1/2}$, and yields an orthorhombic structure with space group *Pnma* and lattice parameters $a_J = 7.33$, $b_J = 6.42$, and $c_J = 7.14$ Å. MDO2 results from the $2_{1/2}|2_{1/2}|2_{1/2}$... sequence of symmetry operators and yields a monoclinic structure with space group $P2_1/c$, $a_M = 7.33$, $b_M = 7.14$, $c_M = 7.39$ Å, and $\beta = 119.7°$.

The analysis of one-dimensional stacking disorder was performed by fitting the observed XRPD pattern with a calculated intensity curve generated by DIFFaX. The disorder model was investigated by taking into account a probability matrix for the occurrence of OD layer sequences. The best fit ($R_p = 0.009$) to the observed powder pattern was obtained with a 61:39 ratio of monoclinic and orthorhombic polytypes for a fully disordered OD layers sequence.

INTRODUCTION

The iron sulfate $FeOHSO_4$ was crystallized for the first time by Maus (1827) but the chemical formula he proposed for this compound was shown to be incorrect. Posnjak and Merwin (1922) determined some of the crystallographic and optical features and studied the stability over a limited temperature range of 50 to 200 °C. Synthetic crystals suitable for single-crystal X-ray analysis were obtained and structurally investigated by Johansson (1962). According to this author, the compound forms orthorhombic crystals with lattice parameters $a_J = 7.331(5)$, $b_J = 6.419(5)$, and $c_J = 7.142(5)$ Å [a_J, b_J, and c_J are the lattice parameters measured by Johansson (1962) for the orthorhombic form], space group *Pnma*, and $Z = 4$. The structure contains two crystallographically independent iron atoms, each octahedrally coordinated by four oxygen atoms and two hydroxyl groups. The OH^- groups are shared between two adjacent Fe-octahedra which are connected to each other to form chains, of $\{\ldots Fe(OH)O_2\ldots\}$ composition, running parallel to **a**. The four octahedral O atoms are shared with sulfate tetrahedra. They provide connectivity between the Fe-chains to make up a three-dimensional network which is based on $[Fe^{3+}O_4(OH)_2]^{7-}$ octahedra and $[SO_4]^{2-}$ tetrahedra. Recently, $FeOHSO_4$ has received a lot of attention because its thermal decomposition and hydrolysis products are important for industrial application such as pigments, catalysis, and magnetic materials. Several studies (Mahapatra et al. 1990; Pelovski et al. 1996 and references therein) have been carried out on the quoted compound with different techniques and methods (derivatographic, thermogravimetric, powder X-ray phase analysis, and Mössbauer spectroscopy) with the aim of acquiring a deep knowledge of its stability, synthesis in various gaseous environments, and finally to investigate its behavior in the dehydration processes.

The sample used for this study has been identified as a high-temperature phase derived from a metahohmannite compound during a synchrotron real-time powder diffraction experiment. In fact at about 100 °C hohmannite $Fe_2(H_2O)_4[O(SO_4)_2]\cdot 4H_2O$ transforms to metahohmannite $Fe_2^{3+}(H_2O)_4[O(SO_4)_2]$ releasing

* E-mail: f.scordari@geomin.uniba.it

almost instantly all the interstitial water molecules (Césbron 1964; Scordari et al. 2004). At higher temperature, about 190 °C, the decomposition of metahohmannite begins, producing by solid-state reaction the ferric-hydroxysulfate compound studied here.

In situ synchrotron X-ray diffraction combined with Rietveld analysis is the best experimental tool for following in detail the temperature-induced solid-state transformation and for providing insight into the dehydration mechanisms and structural changes taking place upon heating.

The Rietveld refinement of the pattern at 220 °C beginning with the structural model of Johansson (1962) was unsuccessful and suggested that the dehydration product of metahohmannite could present order-disorder (OD) character. Recognition of OD character, and the solution and refinement of the disordered structures, is a consonant practice with single crystal X-ray diffraction techniques (Merlino 1990a, 1990b, 1997; Kampf et al. 2003). In the case of powder data, the reduced information content compared to single-crystal analysis makes it rather complicated to model the structural disorder. Nevertheless, in the last few years the development of modeling methods makes it possible to determine both the nature and quantity of structural disorder in XRPD patterns. The diffraction effects in the case of planar disorder can be successfully treated using a recursion algorithm implemented in the program DIFFaX (Treacy et al. 1991) and the occurrence and model of disorder can be extracted from a high resolution X-ray powder pattern (Artioli et al. 1995; Gualtieri 1999; Muller et al. 1999; Viani et al. 2002). The program DIFFaX is based on a rigorous recursion method (Michalsky, 1988; Michalsky et al. 1988) for the generation of random stacking sequences modeling the presence of planar faults. The program allows the calculation of the incoherent sum of scattered intensities from a finite ensemble of layers stacked along a particular direction. A probability matrix for the occurrence of different layer sequences is taken into account, and the extensive planar disorder is described using a mathematical model (Hendricks and Teller 1942; Wilson 1943; Allegra 1964; Kakinoki and Komura 1965; Kakinoki 1967). The details of the algorithm and the theoretical aspects are described in Treacy et al. (1991).

In this paper, using the OD approach (Dornberger-Schiff 1964, 1966; Dornberger-Schiff and Fichtner 1972; Ďurovič 1997; Merlino 1997; Ferraris et al. 2004), we describe the peculiar features of the observed powder pattern in terms of the OD character of the structure, discuss the "superposition structure" of the OD family, and derive the possible MDO polytypes. It shows that they are only two: MDO1 (previously discussed by Johansson 1962) and MDO2, described here for the first time. The proposed one-dimensional disorder model was evaluated by fitting a calculated intensity curve, generated by DIFFaX, to the observed X-ray powder diffraction pattern. In addition, the powder patterns of the two polytypes were generated by DIFFaX and are presented here.

Experimental methods

The investigated iron sulfate $FeOHSO_4$ was obtained by heating metahohmannite during a phase-transformations study of a sample of hohmannite from Northern Chile. The crystal chemical formula assigned to both compounds according to structural results were $Fe_2(H_2O)_4[O(SO_4)_2]$ and $Fe_2(H_2O)_4[O(SO_4)_2]\cdot 4H_2O$ respectively (Scordari 1978; Scordari et al. 2004). Intensities for the structure solution were collected during a synchrotron real-time powder diffraction experiment performed at the Italian beamline BM8 at ESFR (Grenoble, France). The BM8 beamline geometry is described in detail by Meneghini et al. (2001). The capillary (0.5 mm diameter) sample was mounted on a standard goniometer head and kept spinning during the data collection in parallel-beam Debye geometry. A monochromatized fixed wavelength of 0.68881 Å was employed and calibrated with FIT2D (Hammersley 1998) against an Si standard NBS-640b with $a = 5.43094(4)$ Å at 298 K.

Temperature-resolved experiments were performed by continuous heating of the sample in the range 20–800 °C using a heating gun. The temperature was monitored with a thermocouple positioned about half a millimeter below the capillary. Two dimensional diffraction circles were recorded with an imaging-plate (IP) detector (Amemija 1990) mounted perpendicular to the incoming beam at a distance of 257 mm. The IP detector was mounted on a translating system (TIPS: Norby 1996; Meneghini et al. 2001) behind a steel screen with a vertical 3 mm slit and the heating rate of the experiment was synchronized with the speed of the translating system. The image stored in the IP was recovered using a Molecular Dynamics scanner with a dynamical range of 16 bit/pixel and a minimum pixel size of 50×50 μm^2 (Fig. 1a). Slices of intensity representing a specified temperature range, encompassing about 11 K each, were extracted from the stored digitalized file using a specially developed program SCANTIME for the extraction of powder patterns (see the 3-dimensional 2θ-intensity-temperature pattern in Fig. 1b).

Structure refinement

The present study is part of a general project on phase transformations involving iron hydrated sulfates formed by temperature-induced dehydration reactions, using in situ time-resolved synchrotron powder diffraction. Scordari et al. (2004) studied the phase transition hohmannite → metahohmannite and solved the crystal structure of the latter by profile deconvolution and the application of standard Patterson and difference Fourier

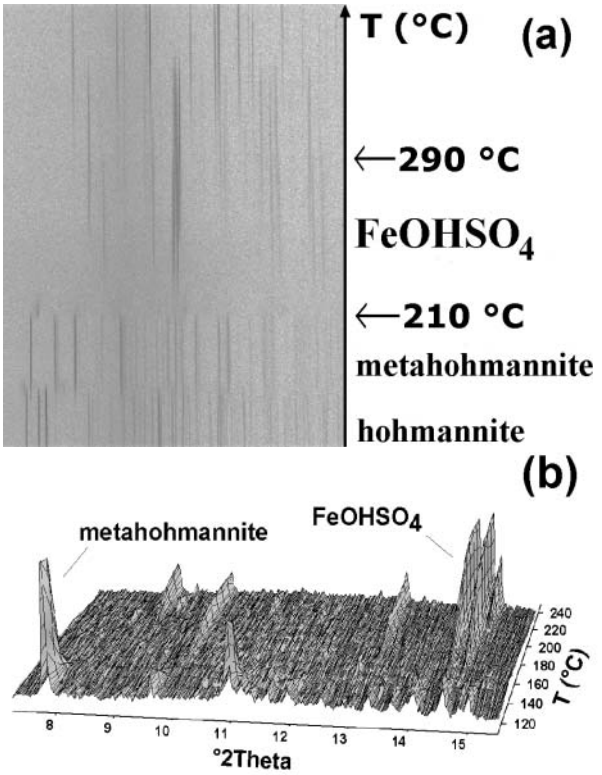

Figure 1. The image obtained from the IP (**a**) and the three-dimensional plot (2θ-intensity-temperature) extracted by integration in the direction normal to the IP translation (**b**). The 7–15.5 °2θ region is reported in the temperature range 120–240 °C.

maps. This work is focused on the structural response of metahohmannite to a temperature-induced transition, particularly the structural details of the new phase that originates from it. Hohmannite, $Fe_2(H_2O)_4[O(SO_4)_2]\cdot 4H_2O$, and metahohmannite, $Fe_2(H_2O)_4[O(SO_4)_2]$, are based on the same centrosymmetric chain with ($Fe_4(H_2O)_8[O_2(SO_4)_4]$) composition. Thus, they differ only for the water content and consequently for the hydrogen bond system of their structure.

Our synchrotron X-ray diffraction data showed that at about 190 °C the overall intensity of the metahohmannite diffraction pattern started to decrease, suggesting that some metahohmannite was decomposing. The decline in overall peak intensities with growing temperature continued up to the disruption of this compound, which occurred at about 210 °C. At higher temperature a new phase became visible (~220 °C) that remained stable up to at least 290 °C, where the first $FeSO_4$ diffraction peaks appeared. To sum up, the reaction sequence obtained from thermal decomposition of hohmannite in the range 20-290 °C, is:

$$\underset{(Fe_2(H_2O)_4[O(SO_4)_2]\cdot 4H_2O)}{\text{hohmannite}} \rightarrow \underset{(Fe_2(H_2O)_4[O(SO_4)_2])}{\text{metahohmannite}} \rightarrow$$

$$\underset{(Fe - H_2O - SO_4)}{\text{amorphous phase}} \rightarrow \underset{(FeOHSO_4)}{\text{synthetic phase}}$$

These solid-state transformations are easily explained if the structure of the quoted compounds is taken into account. During the transformation hohmannite → metahohmannite, only the structural water is involved in the reaction (4 H_2O, lost/regained). Therefore, in the presence of water, this reaction is simple and reversible. As a consequence, the backbone of the structure, i.e., the ($Fe_2(H_2O)_4[O(SO_4)_2]$) chain, should be topologically unchanged in both the hohmannite and metahohmannite structures. The next reaction, metahohmannite → $FeOHSO_4$, is quite different. In fact, metahohmannite should lose three water molecules directly coordinated by Fe^{3+} cations to form the more stable compound. This triggers the breakdown of the ($Fe_2(H_2O)_4[O(SO_4)_2]$) chains and the consequent formation of an intermediate amorphous phase from which the $FeOHSO_4$ compound later forms. The first reaction (hohmannite to metahohmannite) is certainly topotactic whereas the formation of $FeOHSO_4$ is a typical nucleation and growth reaction process.

Theses observations seem to be consistent with the results of the differential thermal analysis (DTA) of hohmannite samples performed by Césbron (1964). According to this author one sharp and one large peak are visible at about 120 and 240 °C, in keeping with the hohmannite → metahohmannite and metahohmannite → $FeOHSO_4$ transformation temperatures observed here. In addition, the $FeOHSO_4$ structure is completely destroyed at about 500 °C, in agreement with the stability studies carried out by Pelovski et al. (1996).

A full-profile Rietveld refinement of the $FeOHSO_4$ material formed during the heating experiment was performed with GSAS (Larson and Von Dreele 2000). The starting lattice and atomic parameters for the 220 °C pattern refinement were taken from Johansson (1962). The refinement parameters included the scale factor and 14 background terms in a Chebyshev polynomial function. Peak profiles were modeled using a pseudo-Voigt function with three Gaussian and two Lorentzian line-broadening terms. During refinement of the atomic positions in the space group *Pnma*, soft constrains to the S-O and Fe-O distances were applied, and the weighting factor was gradually reduced in successive cycles. Unfortunately, the refinement did not yield an R_p value below 22.8%. Thereafter we carefully analyzed the features of the powder diffraction pattern and we observed that the experimental powder pattern was quite different from that calculated (Fig. 2) using the parameters and atomic positions given by Johansson (1962).

In particular we noticed:

(1) unexpected absences for reflections with $h = 2n + 1$, indicated by stars in the powder pattern; and

(2) indexing of the pattern using the program Treor99 (Werner et al. 1985) indicated an orthorhombic cell with lattice parameters $a_J' = 3.6677(1)$, $b_J' = 6.4176(1)$, and $c_J' = 7.1590(2)$ Å. Moreover, taking into account these lattice parameters, systematic absences were observed corresponding to a body centered cell and pointing to the space group *Immm* (see Table 1). On the contrary, if Johansson lattice parameters are used, some calculated powder pattern peaks are not seen in the experimental pattern (marked by stars in Table 2).

In addition, forewarning about the OD character of the $FeOHSO_4$ structure also arises from the existence in the 1995 edition of Powder Diffraction File (PDF) of more than one data set concerning the quoted compound with lines corresponding to the same observed *d* values, but with some relative intensities in disagreement with our observed pattern (Fichtner 1979).

TABLE 1. Powder pattern indexed with a_J', b_J', and c_J' parameters in the range 7–20°(2θ)

h	*k*	*l*	*d* (Å)	I_{rel}
0	1	1	4.774	24.6
0	0	2	3.570	26.9
1	0	1	3.261	100
0	2	0	3.210	72.1
1	1	0	3.183	< 1
0	2	2	2.387	< 1
1	1	2	2.376	3.8
1	2	1	2.288	13.4
0	1	3	2.232	13.8
0	3	1	2.050	13.6
1	0	3	1.996	13.1

TABLE 2. Powder pattern indexed with a_J, b_J, and c_J parameters in the range 7–20 °2θ

h	*k*	*l*	*d* (Å)	I_{rel}
1	0	1	5.115	16.1*
0	1	1	4.770	19.2
1	1	1	3.998	16.4*
0	0	2	3.570	28.7
2	0	1	3.261	100
0	2	0	3.210	78.7
2	1	0	3.182	12.8
1	1	2	2.870	18.4*
1	2	1	2.716	4.9*
0	2	2	2.385	2.2
2	1	2	2.375	3.2
3	0	1	2.312	1.4*
2	2	1	2.286	14.4
1	2	2	2.268	9.6
0	1	3	2.231	14.8
3	1	1	2.175	1.1*
0	3	1	2.047	11.9
2	0	3	1.996	12.7
3	1	2	1.923	2.7*

* Reflections with $h = 2n + 1$ not present in the experimental pattern.

These facts confirmed the hypothesis that order-disorder phenomena were active in the structure of the examined compound. As discussed in the next section, in the light of the OD theory the observed powder pattern is the product of a "superposition structure" which arises from the OD character of the compound. Although the reliability is only indicative, the application of direct methods (Altomare et al. 1999) using space group *Immm* resulted in a fictitious structure (R_F = 13.3%) in agreement with the OD theory. A new Rietveld refinement was successfully performed with the same criteria discussed above for the last structural model. The best fit with R_p = 4.77% was obtained for the pattern at 220 °C.

Details of the data collection and structure refinement are included in Table 3. The final fractional coordinates and equivalent isotropic displacement parameters for the "superposition structure" are reported in Table 4, while the interatomic distances are shown in Table 5. The final observed, calculated, and difference powder diffraction patterns resulting from the Rietveld refinement are plotted in Figure 3.

TABLE 3. Crystal data and Rietveld refinement parameters at T = 220 °C

Formula sum	$Fe_4S_8O_{24}H_4$
Formula weight	675.67
Crystal system	orthorhombic
Space group	*Immm*
Unit cell dimensions	a = 3.668(1) Å
	b = 6.418(1) Å
	c = 7.159(1) Å
Cell volume	168.51(1) Å^3
R_{wp}(%) = 6.18	
R_p(%) = 4.77	
Reduced χ^2 = 190.6	$R(F^2)$(%) = 6.44

TABLE 4. Atomic coordinates and isotropic displacement parameters (in Å^2)

Atom	Wyckoff	x	y	z	U_{iso}
Fe	2*e*	0.000	0.000	0.000	0.013(3)
S	4*j*	0.000	0.500)	0.881(1)	0.028(4)
O1	4*g*	0.000	0.683(1)	0.000	0.023(4)
O2	8*m*	0.170(1)	0.000	0.264(1)	0.023(4)
O4	4*j*	0.000	0.500	0.401(1)	0.023(4)

TABLE 5. Selected geometric parameters (Å)

Fe-O1	2.035 (3)	S-O1	1.451(2)
Fe-O2	1.993 (3)	S-O2	1.473 (4)
Fe-O4	1.970 (2)		

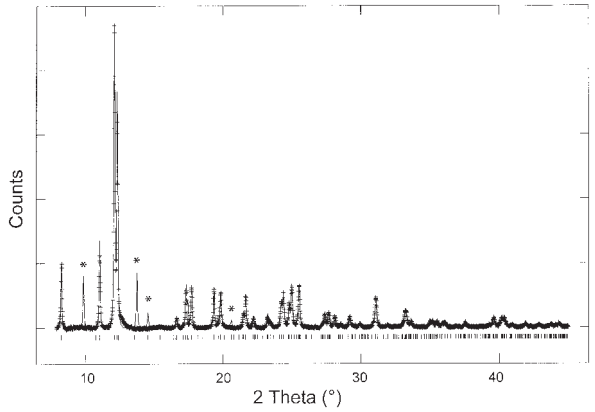

FIGURE 2. Comparison between the diffraction pattern calculated from the data of Johansson (1962) and our experimental data. The stars indicate the unobserved reflections.

OD CHARACTER OF FEOHSO$_4$

In this section we show that all the quoted pattern features may be easily explained in terms of OD theory. Let us consider the unit cell of FeOHSO$_4$ determined by Johansson (1962) seen along $\mathbf{c}_J$ in Figure 4a. To give a more complete representation of the structure projected along $\mathbf{b}_J$ more unit cells need to be considered (Fig. 4b). From inspection of Figure 4b it is easy to see that two different ways of connecting adjacent neighboring layers are possible. The first is shown in Figure 4b. The second can be obtained by shifting the upper layer by a/2 with respect to that immediately below. Combinations of the two stacking sequences make it possible to obtain a family of structures with variable degree of order, and then a family of OD structures.

For a clear and complete description of an OD family, the metrics and symmetry of the OD layer (λ-operations) as well as the operators which bring a layer into coincidence with an adjacent layer (σ-operations) should be considered. These operations are called partial operations (POs) in the OD terminology, since they are not necessarily valid for the whole structure. The symbols for these operators are in keeping with the symbols used in normal space groups.

To obtain an OD groupoid family symbol consistent with that indicated in the basic compilation of Dornberger-Schiff and Fichtner (1972), the $\mathbf{a}_J$, $\mathbf{b}_J$, and $\mathbf{c}_J$ axes of the single layer must be interchanged with respect to those assumed by Johansson (1962). With this interchange the basic OD layer in FeOHSO$_4$ seen along **a** has translation periods a (c_J) and b (a_J), and width c_0, one half of the b_J translation of the orthorhombic cell and symmetry defined by the layer group *Pbmm* (see Fig. 5).

The OD-groupoid symbol is the following:

$$P \quad b \quad m \quad (m)$$
$$\{2_r/n_{s-1,2}\ 2_{s-1}/n_{2,r}\ (2_2/n_{r,s})\}$$

The first and the second lines of the groupoid symbol indicate the λ- and σ-POs respectively, and the round brackets indicate the direction of missing periodicity. For the present case r = 1 and s = 1/2.

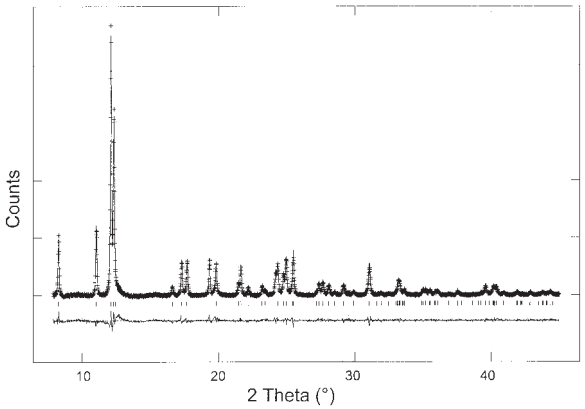

FIGURE 3. Rietveld refinement results for the FeOHSO$_4$ compound. The crosses represent the observed data points, and the smooth line through them the calculated pattern. The different pattern is plotted at the same scale as the other patterns. The row of tick marks indicates the calculated reflection positions.

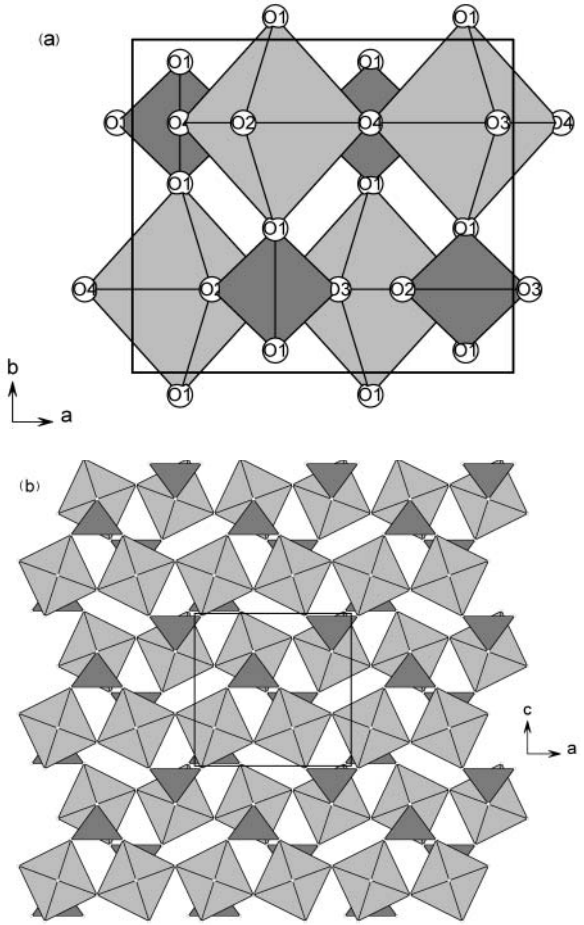

FIGURE 4. The crystal structure of $FeOHSO_4$, studied by Johansson (1962) projected along **c** (a) and **b** (b).

With the new cell setting, layers can be stacked along **c** according to either of the two stacking operators $2_{+1/2}$ and $2_{-1/2}$ parallel to **b**. Pairs of layers related by either of the two operations are geometrically equivalent. Different sequences of operators $2_{+1/2}$ and $2_{-1/2}$ give rise to different structures, actually an infinite number of polytypes, as well as disordered structures, corresponding to ordered or disordered sequences of $2_{+1/2}$ and $2_{-1/2}$ operators. The symmetry of each possible polytype may be derived from the symmetry properties of the family embodied in the OD-groupoid family symbol. Among all possible ordered stacking sequences, there are two in which not only couples, but also triples (quadruples,…,n-ples) of adjacent layers are geometrically equivalent. These are the so-called MDO (Maximum Degree of Order) structures. Focusing on the layer shown in Figure 5, we have only two possible MDO polytypes: (1) MDO1 (Fig. 6) results from a regular alternation of $2_{+1/2}$ and $2_{-1/2}$ stacking operators. In this case an orthorhombic structure is obtained with lattice parameters $a_J = 7.331(5)$, $b_J = 6.419(5)$, and $c_J = 7.142(5)$ Å and space group *Pnma* (the compound studied by Johansson 1962); (2) MDO2 (Fig. 7) results if $2_{-1/2}$ is invariably followed by $2_{-1/2}$; in this case a monoclinic (M) structure is obtained with lattice parameters $a_M = 7.33$, $b_M = 7.14$, and $c_M = 7.39$ Å, $\beta = 119.7°$ and space group $P2_1/c$. Calculated atomic coordinates

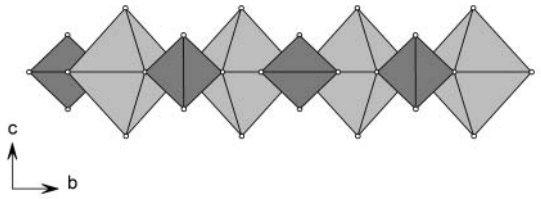

FIGURE 5. Projection along **a** of the single layer characteristic of all $FeOHSO_4$ crystals belonging to the OD family.

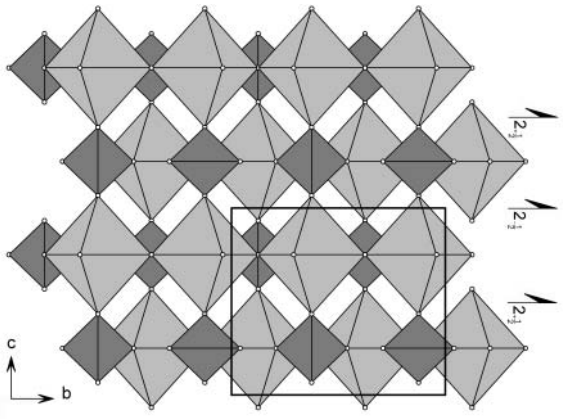

FIGURE 6. Projection along **a** of the MDO1 structure showing the σ-POs and the orthorhombic unit cell.

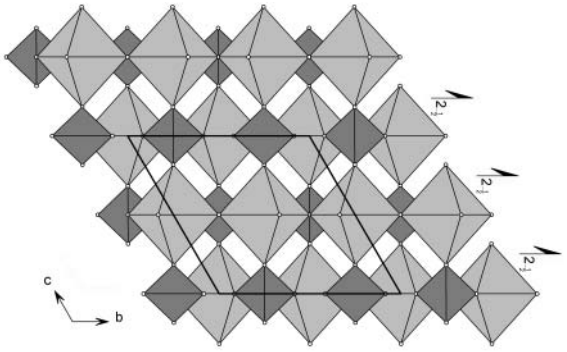

FIGURE 7. Projection along **a** of the MDO2 structure showing the σ-POs and the monoclinic unit cell.

are given in Table 6. It seems proper to recall that the structure obtained when $2_{+1/2}$ is constantly followed by $2_{+1/2}$ is no different from the preceding one and corresponds to its (001) twin.

We know that various disordered and ordered structures display powder diffraction patterns with common reflections, "family reflections", which are always sharp and have the same positions and intensities in all the OD structures of the family. The family reflections arise from a fictitious structure, periodic in three dimensions, closely related to the structures of the family and called the "family structure" or "superposition structure".

It seems useful to observe that in $FeOHSO_4$ layers related by $2_{+1/2}$ and $2_{-1/2}$ operators are translationally equivalent and related by the stacking vectors $\mathbf{t_1} = \mathbf{a}/2 + \mathbf{b}/4 + \mathbf{c}/2$ and $\mathbf{t_2} = \mathbf{a}/2 - \mathbf{b}/4 + \mathbf{c}/2$, respectively. Therefore in general adjacent layers may be described as being related by vectors

TABLE 6. Atomic coordinates of the MDO2 polytype*

Atom	Wyckoff	*x*	*y*	*z*
Fe1	2*a*	0.000	0.000	0.000
Fe2	2*b*	0.5	0.5	0.5
S	4*e*	0.25	0.616	0.0
O1	4*e*	0.3415	0.5	0.183
O2	4*e*	0.916	0.270	0.0
O3	4*e*	0.584	0.270	0.0
O4	4*e*	0.25	0.100	0.0
O5	4*e*	0.8415	0.0	0.683

*The symmetry and the cell parameters of the MDO2 polytype are: space group $P2_1/c$, a_M = 7.33, b_M = 7.14, and c_M = 7.39 Å, and β = 119.7°.

$$\mathbf{t_p} = \mathbf{a}/2 \pm \mathbf{b}/4 + \mathbf{c}/2 \quad (1)$$

By using Equation 1 and following the procedures described in Merlino (1990a, 1997) the Fourier transform of the structure is

$F(hkl) = S(hkl)F_0(hkl)$ with $F_0(hkl)$ the Fourier transform of the L_0 layer and

$$S(hkl) = \sum_p \exp\{2\pi i[(\tfrac{h}{2} + \tfrac{k}{4} + \tfrac{l}{2})p + \mathrm{m}_p \tfrac{k}{2}]\} \quad (2)$$

with m_p and p as integers.

For $k = 2n$ Equation 2 becomes

$$S(hkl) = \sum_p \exp\{(2\pi i(\tfrac{2h+k+2l}{4})p)\} \quad (3)$$

With many layers (p) this expression vanishes except for

$$2h + k + 2l = 4n \quad (4)$$

These reflections correspond to a reciprocal lattice with vectors $\mathbf{A}^*$ $\mathbf{B}^*$ and $\mathbf{C}^*$ which are related to the basic vectors $\mathbf{a}^*$ $\mathbf{b}^*$ $\mathbf{c}^*$ as follows:

$$\mathbf{A}^* = \mathbf{a}^*, \mathbf{B}^* = 2\mathbf{b}^*, \mathbf{C}^* = \mathbf{c}^* \quad (5)$$

Therefore, for these reflections Equation 4 becomes: $h + k + l = 2n$, which points to an *I* lattice.

Assuming two basis vectors of the family structure collinear with the translation vectors **a** and **b** of the single layer, the vectors **A B C** of the family structure are such that: $\mathbf{a} = t\mathbf{A}$, $\mathbf{b} = q\mathbf{B}$, and $\mathbf{C} = p\mathbf{c}_0$, where q, t, and p are integers.

From Equation 5 we obtain $\mathbf{a} = \mathbf{A}$ and $\mathbf{b} = 2\mathbf{B}$; therefore $q = 2$ and $t = 1$.

The number of layers, p, for each *C* translation of the "family structure" may be obtained as the product of three factors $p = p1p2p3$ (Dornberger-Schiff and Fichtner 1972), where $p1$ depends on the category of the OD structure, $p2$ depends on the isogonality relationships of operations in the OD-groupoid family symbol, and $p3$ depends on the Bravais lattice of the family structure (Ďurovič 1997; Ferraris et al. 2004). In the case under study we have category *I* ($p1 = 1$), isogonality ($p2 = 1$), and *I* centering ($p3 = 2$). As a consequence $p = 2$.

Therefore the symmetry operations of the family structure may be obtained from the POs presented in the OD groupoid symbol of the family

$P \quad 2/b \quad 2_1/m \quad (2/m)$
$\{2_1/n_{1/2}\ 2_{-1/2}/n_{2,1}\ (2_2/n_{1,1/2})\}$

by doubling the translational components which refer to **b** and divide by two the translational components which refer to **c**. The symmetry operations thus obtained exactly correspond to those of space group *Immm*. It is therefore confirmed that the family structure has *Immm* symmetry with $a = 7.142$, $b = 3.66$, and $c = 6.419$ Å.

Order-disorder model

According to the conclusions from the application of the OD theory, $FeOHSO_4$ belongs to a family of OD structures made up of equivalent layers. Regular sequences of stacking vectors between layers yield ordered structures, and, in particular, only two MDO polytypes: orthorhombic MDO1 and monoclinic MDO2. Disordered sequences of stacking vectors yield one-dimensionally disordered structures. The program DIFFaX was applied to simulate the XRPD patterns of these two polytypes. Because the program requires that **c** be parallel to the stacking direction, the unit layer and the same axes setting applied in the OD section were used. If domains of MDO1 polytype are present, they are characterized by a regular alternation of stacking vectors $\mathbf{t_1} = \mathbf{a}/2 + \mathbf{b}/4 + \mathbf{c}/2$ and $\mathbf{t_2} = \mathbf{a}/2 - \mathbf{b}/4 + \mathbf{c}/2$, while the MDO2 polytype domains are characterized by a regular sequence of stacking vector $\mathbf{t_1}$ (or $\mathbf{t_2}$) and $\mathbf{t_1}$ and $\mathbf{t_2}$ for the (001) twinned case. However, the coexistence of domains of both polytypes would cause, besides the "family reflections," weak and diffuse reflections that are not observed in the experimental powder pattern (see Figs. 2–3).

We employed a pseudo-Voigt function to describe the intensity distribution of the Bragg peaks due to instrumental and sample effects. A cross-check of the consistency of the simulated powder patterns was performed by comparing the diffraction profile from DIFFaX with other programs (GSAS) showing that the two patterns (Figs. 8–9) were in excellent agreement. It seems proper to remark that the powder pattern of the two polytypes exhibit close analogies ("family reflections"), as well as significant differences.

From the comparison of the experimental and simulated patterns it is clear that the observed reflections correspond to "family reflections," and reflections characteristic of the two individual polytypes are missing. This rules out the existence of coherent diffracting domains of individual polytypes and points to a random sequence of the polytypes indicative of an extensive stacking disorder in the structure. Such a random sequence can only be simulated using DIFFaX which takes advantage of the recursive method. The matrix method implemented in the program DIFFaX was applied to calculate the intensity distribution in powder X-ray diffraction patterns of $FeOHSO_4$, taking into account a probability matrix for the occurrence of different layer sequences.

The full description of disorder in each simulation implies a square probability matrix of order n (with n equal to the number of crystallographically distinct layers), where each element a_{ij} refers to the probability of stacking layer j over layer i in the sequence. A disorder model of Reichweite $R = 1$ was handled by using four different layers. The term Reichweite was introduce by Jagodzinski (1949a, 1949b, 1949c) and defines the range of interaction between the arrangement of neighboring layers. In this simple case, only next-nearest interactions are considered. Layer 1 and 3 are characterized by a **b**/2 translation, and layers 2 and 4 by a –**b**/2 translation. By gauging the matrix elements, we can control the interaction probability between any two layers in the structure, and at the same time evaluate the volume ratio of orthorhombic to monoclinic domains.

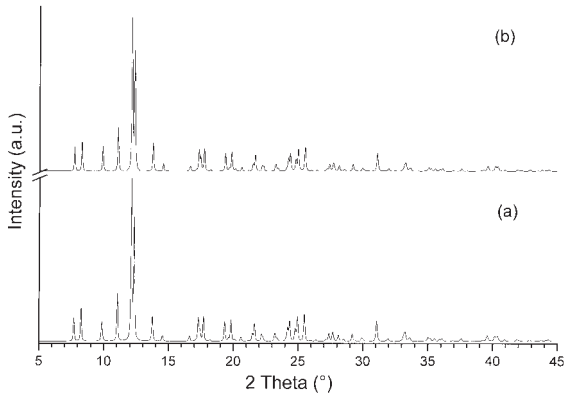

FIGURE 8. Simulated powder patterns of the MDO1 structure of $FeOHSO_4$ calculated with (**a**) DIFFaX and (**b**) GSAS.

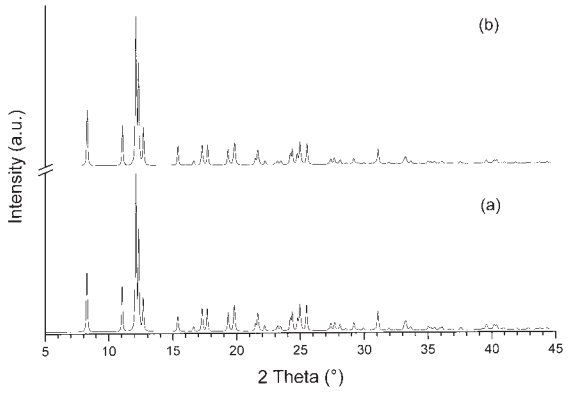

FIGURE 9. Simulated powder patterns of the MDO2 structure of $FeOHSO_4$ calculated with (**a**) DIFFaX and (**b**) GSAS.

Therefore, as shown in Figure 10, α_{11} and α_{44} represent the probability of occurrence of monoclinic domains characterized by a stacking sequence of vectors $\mathbf{t_1}$ and $\mathbf{t_2}$ respectively, whereas α_{23} (= α_{32}) represents the probability of occurrence of orthorhombic domains characterized by regular stacking alternation of vectors $\mathbf{t_1}$ and $\mathbf{t_2}$.

We interpret the statistical probability indicated by α_{12} (= α_{43}) and α_{24} (= α_{31}) matrix elements to be related to the crystallochemical probability of faulting in the monoclinic (orthorhombic) domains. The stacking transitions α_{13}, α_{14}, α_{21}, α_{22}, α_{33}, α_{34}, α_{41}, and α_{42} cannot occur by definition.

When the faulting is random the stacking transition probabilities follow the relations:

$$\alpha = \alpha_{11} = \alpha_{44} = \alpha_{24} = \alpha_{31} = 1 - \alpha_{12} = 1 - \alpha_{23} = 1 - \alpha_{32} = 1 - \alpha_{43}.$$

A fully ordered orthorombic structure is obtained for $\alpha = 0.00$. With increasing probability α the volume fraction of monoclinic layer sequences increases (Fig. 11). The calculated patterns were compared to the observed one. The background was manually removed, the zero-shift corrected, and the scale factor was varied to obtain the best fit. The best fit to the observed powder pattern was obtained with $\alpha = 0.61$ (Fig. 12) with the final agreement ($R_p = 0.009$) evaluated using the factor:

$$R_p = \{\Sigma[y_i(\text{obs}) - y_i(\text{calc})]^2\} / \Sigma[y_i(\text{obs})]^2$$

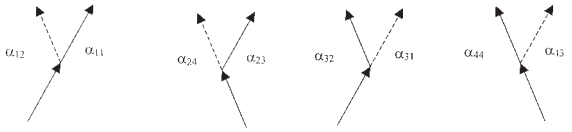

FIGURE 10. Diagram illustrating the transition rules implemented in DIFFaX.

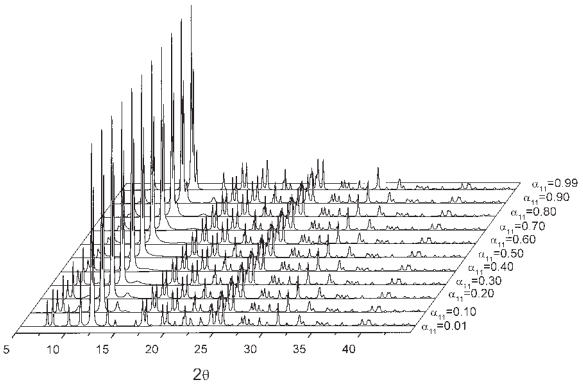

FIGURE 11. Montage of powder X-ray diffraction patterns calculated as a function of the probability of monoclinic stacking. Instrumental peak broadening was simulated using a pseudo-Voigt function. The step size was 0.01 °2θ.

The monoclinic form seems to be slightly favored although the close similarity of the stacking sequence of the two different polytypes should indicate a nearly identical activation energy for their formation. Although it is not possible here to ascertain if a different polytypic sequence could be obtained using different kinetic conditions, the formation of an OD structure instead of a single polytype opens a debate on the stability of the OD structure. Is the existence of an OD character simply a kinetic effect due to the fast heating rate of the experiment (that is, the OD structure is actually a metastable phase and the precursor of a stable polytype), or is the OD-structure a stable phase?

There is clear evidence to support the latter statement. First of all, looking at the sequence of powder patterns with increasing temperature, the peaks of the OD structure are nearly unchanged up to about 500 °C, where, in concert with the stability studies carried out by Pelovski et al. (1996), the structure is destroyed. The fact that no transitions or transformations are observed in such a large temperature interval is a good indication that the OD phase is stable. In addition, the existence of an OD structure instead of a single polytype was evident to Johansson (1962) who reported the same order of problems during the crystal structure solution of two Fe^{3+} and In^{3+} sulfates. As a matter of fact, Johansson found that the $R(Fo)$ factor was worse (from 7–8% to about 11–13%) when reflections with h odd were included in the refinement. He also reported that "*difficulties were encountered in finding good single crystals of the corresponding indium compound. The spots on the Weissenberg films were often extended and diffuse* (typical of a disordered sequence) *and showed very weak reflections hk0 for h odd*." This shows that both the compounds synthesized by Johansson were affected by stacking disorder and likely displayed an OD-structure despite the very different kinetic conditions of crystallization. In fact, it is important to remark that the conditions of synthesis reported by Johansson (1962), a $Fe_2O_3 + SO_3$

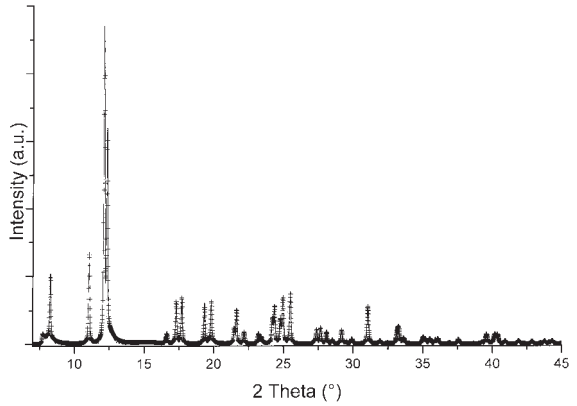

FIGURE 12. Comparison of calculated XRPD pattern (solid lines) with the observed one (crosses). The fit is best (R_p = 0.009) for α = 0.61. Instrumental peak broadening was simulated using a pseudo-Voigt function. The step size was 0.01 °2θ.

rich solution heated at 200 °C for a month, a period long enough to indicate that equilibrium—or close to equilibrium—conditions should have been obtained, are very different from the ones reported here, again indicating that the formation of the OD-structure is not simply determined by the reaction kinetics. Thus, if we rule out a kinetic factor for the formation of this OD structure, it is reasonable to state that for both structural and energetic reasons, the OD structure is stable and that the monoclinic and the orthorhombic polytypes can occur simultaneously, leading to a structure with stacking disorder.

ACKNOWLEDGMENTS

C. Dalconi and G. Cruciani are acknowledged for their help with the data reduction and useful discussions. We also thank J. Hanson and S. Merlino for their reviews together with R. Downs for suggestions that greatly improved the manuscript.

REFERENCES CITED

Allegra, G. (1964) The calculation of the intensity of X-rays diffracted by monodimensionally disordered structures. Acta Crystallographica, 17, 579–586.

Altomare, A., Burla, M.C., Camalli, M., Carrozzini, B., Cascarano, G., Giacovazzo, C., Guagliardi, A., Moliterni, A.G.G., Polidori, G., and Rizzi, R. (1999) EXPO: a program for full powder pattern decomposition and crystal structure solution. Journal of Applied Crystallography, 32, 339–340.

Amemija, Y. (1990) Imaging plate—X-ray area detector based on photostimulable phosphor. Synchrotron Radiation News, 3, 21–26.

Artioli, G., Bellotto, M., Gualtieri, A.F., and Pavese, A. (1995) Nature of structural disorder in natural kaolinites: a new model based on computer simulation of powder diffraction data and electrostatic energy calculation. Clays and Clay Minerals, 43, 438–445.

Césbron, F. (1964) Contribution à la Minéralogie des sulfates de fer hydratés. Bulletin Societe Francais de Mineralogie et Crystallographie, 87, 125–143.

Dornberger-Schiff, K. (1964) Grundzüge einer Theorie von OD-Strukturen aus Scjhikten. Abhandlungen der deutschen Akademie der Wissenschaften zu Berlin, Klasse für Chemie, Geologie und Biologie, Jahrgang 1964 Nr. 3, 1–107.

——— (1966) Lehrgang über OD structuren. Berlin: Akademie-Verlag, 135 p.

Dornberger-Schiff, K. and Fichtner, K. (1972) On the symmetry of OD-structures consisting of equivalent layers. Kristall und Technik, 7, 1035–1056.

Ďurovič, S. (1997) Fundamentals of OD theory. In S. Merlino, Ed., Modular aspects of minerals, 1, 3–28. EMU Notes in Mineralogy, Eötvös University press, Budapest, Hungary.

Ferraris, G., Makovicky, E., and Merlino, S. (2004) Crystallography of Modular Materials. IUCr Monographs on Crystallography, 15. Oxford University Press, New York.

Fichtner, H.S. (1979) On some features of X-ray powder patterns of OD structures. Kristall und Technik, 14, 1079–1088.

Gualtieri, A.F. (1999) Modelling the nature of disorder in talc by simulation of X-ray powder patterns. European Journal of Mineralogy, 11, 521–532

Hammersley, A.P. (1998) FIT2D V10.3 Reference Manual V4.0 ESRF98HA01T.

Hendricks, S. and Teller, E. (1942) X-ray interference in partially ordered layer lattices. Journal of Chemical Physics, 10, 147–167.

Jagodzinski, H.(1949a) Eindimensionale Fehlordnung in Kristallen und ihr Einfluβ auf die Röntgeninterferenzen. I, Berechnung des Fehlordnungsgrades aus den Röntgenintesitäten. Acta Crystallographica, 2, 201–207.

Jagodzinski, H.(1949b) Eindimensionale Fehlordnung in Kristallen und ihr Einfluβ auf die Röntgeninterferenzen. II, Berechnung des Fehlgeordneten dichtesten Kugelpackungen mit Wechselwirkungen der Reichweite 3. Acta Crystallographica, 2, 208–214.

Jagodzinski, H.(1949c) Eindimensionale Fehlordnung in Kristallen und ihr Einfluβ auf die Röntgeninterferenzen. III, Vergleich der Berechnung mit experimentellen Ergebnissen. Acta Crystallographica, 2, 298–304.

Johansson, G. (1962) On the crystal structure of $FeOHSO_4$ and $InOHSO_4$. Acta Chemica Scandinavica, 16, 1234–1244.

Kakinoki, J. (1967) Diffraction by a one-dimensionally disordered crystal. II. Close-packed structures. Acta Crystallographica, 23, 875–885.

Kakinoki, J. and Komura, Y. (1965) Diffraction by a one-dimensionally disordered crystal. I. The intensity equation. Acta Crystallographica, 19, 137–147.

Kampf, A.R., Merlino, S., and Pasero, M. (2003) Order-disorder approach to calcioaravaipaite, $[PbCa_2Al(F,OH)_9]$: The crystal structure of the triclinic MDO polytype. American Mineralogist, 88, 430–435.

Larson, A.C. and Von Dreele, R.B. (2000) General Structure Analysis System (GSAS). Los Alamos National Laboratory Report LAUR 86–748.

Mahapatra, S., Prasad, T.P., Rao, K.K., and Nayak, R. (1990) Thermal decomposition of hydrolysis products of $Fe(OH)SO_4$. Thermochimica Acta, 161, 279–285.

Meneghini, C., Artioli, G., Balerna, A., Gualtieri, A.F., Norby, P., and Mobilio, S. (2001) Multipurpose imaging-plate camera for in-situ powder XRD at the GILDA beamline. Journal of Synchrotron Radiation, 8, 1162–1166.

Maus, A. (1827) Uber einige neue Salze des Eisenoxyds und der Thonerde. XI Annalen der Physik, 75–82 p.

Merlino, S. (1990a) OD structures in Mineralogy. Periodico di Mineralogia, 59, 69–92.

——— (1990b) Lovdarite, $K_4Na_{12}(Be_8Si_{28}O_{72})\cdot 18H_2O$, a zeolite-like mineral: structural features and OD character. European Journal of Mineralogy, 2, 809–817.

——— (1997) OD approach in minerals: examples and applications. In S.Merlino, Ed., Modular aspects of minerals, 1, 3–28. EMU Notes in Mineralogy, Eötvös University press, Budapest, Hungary.

Michalsky, E. (1988) The diffraction of X-ray by close packed polytypic crystals containing single stacking faults. I. General theory. Acta Crystallographica, A44, 640–649.

Michalsky, E., Kaczmarek, S., and Demianiuk, M. (1988) The diffraction of X-ray by close packed polytypic crystals containing single stacking faults. I. Theory for hexagonal and rhombohedral structures. Acta Crystallographica, A44, 650–657.

Muller, F., Plancon, A., Besson, G., and Drits, V.A. (1999) Nature, proportion and distribution of stacking faults in celadonite minerals. Materials Structure, 6, 129–134.

Norby, P. (1996) In situ time-resolved synchrotron powder diffraction studies of syntheses and chemical reactions. Materials Science Forum, 147, 228–231.

Pelovski, Y., Petkova, V., and Nikolov, S. (1996) Study of the mechanism of the thermochemical decomposition of ferrous sulphate monohydrate. Thermochimica Acta, 274, 273–280.

Posnjak, E. and Merwin, H.E. (1922) The system, Fe_2O_3-SO_3-H_2O. Journal of the American Chemical Society, 44, 1965–1994

Scordari, F. (1978) The crystal structure of hohmannite, $Fe_2(H_2O)_4[(SO_4)_2O]\cdot 4H_2O$ and its relationship to amarantite, $Fe_2(H_2O)_4[(SO_4)_2O]\cdot 3H_2O$. Mineralogical Magazine, 42, 144–146.

Scordari, F., Ventruti, G., and Gualtieri, A.F. (2004) The structure of metahohmannite, $Fe^{+3}{}_2[O(SO_4)_2]\cdot 4H_2O$, by in situ synchrotron powder diffraction. American Mineralogist, 89, 265–270.

Treacy, M.M.J., Newsam, J.M., and Deem, M.W. (1991) A general recursion method for calculating diffracted intensities from crystals containing planar faults. Proceedings of the Royal Society of London A, 433, 499–520.

Viani, A., Gualtieri, A.F., and Artioli, G. (2002) The nature of disorder in montmorillonite by simulation of X-ray powder patterns. American Mineralogist, 87, 966–975.

Werner, P.E., Eriksson, L., and Westdahl, M. (1985) TREOR, a semi exhaustive trial-and-error powder indexing program for all symmetries. Journal of Applied Crystallography, 18, 367–370.

Wilson, A.J.C. (1943) The reflection of X-rays from the "anti-phase nuclei" of $AuCu_3$. Proceedings of the Royal Society of London A, 181, 360–368.

MANUSCRIPT RECEIVED JUNE 4, 2004
MANUSCRIPT ACCEPTED JULY 23, 2004
MANUSCRIPT HANDLED BY MICHAEL FECHTELKORD